Basin-Scale Carbon Monoxide Distributions in the Parallel Ocean Program

Shaoping Chu and Scott Elliott*

Climate Ocean Sea Ice Model Project (COSIM), Los Alamos National Laboratory, Los Alamos, New Mexico

David Erickson

Climate Dynamics Group, Computer Science and Mathematics Division, Oak Ridge National Laboratory, Oak Ridge, Tennessee

Received 6 July 2006; accepted 11 January 2007

ABSTRACT: As a primary photochemical constituent in upper-ocean and tropospheric geocycling, carbon monoxide is of interest to a variety of global change research communities. Dynamic three-dimensional simulations of its marine concentration patterns, emphasizing Pacific surface waters, are presented. Calculations were driven by nitrogen/iron ecodynamics within the Parallel Ocean Program (POP) transport framework. Photoproduction was estimated following broadband transfer of ultraviolet A radiation down to and penetrating the mixed layer. Quantum efficiency, absorption, the chromophoric fraction of dissolved organics, and related microchemical parameters were all varied, in some cases collectively. Bacterial uptake was parameterized through stages of refinement ranging from a single global average time constant to the application of steady-state zooplanktonic grazing pressure. Major features of basin-spanning ship track data can be reproduced including tropical to gyre and

* Corresponding author address: Scott Elliott, Mail Stop D413, Los Alamos National Laboratory, Los Alamos, NM 87545.
E-mail address: sme@lanl.gov

DOI: 10.1175/EI211.1

temperate frontal ratios. Evidence for ecosystem structural influence upon the removal kinetics is reviewed and investigated. Polar waters exhibit unique processing modes and the periphery of the ocean requires specialized handling of organic and bacterial behavior. Large-scale budgets are consistent with recent independent determinations both with respect to internal turnover and flux to the atmosphere. A parsimonious mechanism involving optimized yield is recommended for early system model efforts. Areas awaiting improvement include resolution of UV and the segregation of both light-interacting carbon compounds and microbial populations as tracers.

KEYWORDS: Carbon monoxide; Dissolved concentrations; OGCM

1. Introduction

Carbon monoxide is a key component of the oceanic photochemical system and it also influences the oxidizing capacity of the lower atmosphere. Within mixed layer seawater the molecule functions as an intermediate during the photolytic breakdown of dissolved organics (Mopper et al. 1991; Mopper and Kieber 2002). In the gas phase, CO is involved in regulation of the hydroxyl radical (Logan et al. 1981; Crutzen and Zimmerman 1991). Surface ocean contributions to the global atmospheric source are relatively small, but strong local fluxes can elevate concentrations in the boundary layer (Erickson and Taylor 1992; Springer-Young et al. 1996). Overall, the compound may be viewed as a primary tracer of photoreaction activity both below and above the sea surface.

While large-scale sea–air transfer and ocean internal budgets have been computed and offered several times in the literature (Bates et al. 1995; Zafiriou et al. 2003), dynamic simulation of marine CO geocycling is currently in its infancy. Attempts have been made to capture major features of depth profile evolution in analytical or low-dimensionality models (Johnson and Bates 1996; Kettle 2000). The production field has been reconstructed based on ship track data (Zafiriou et al. 2003) or the inversion of organic optical behavior from satellite color instruments (C. Fichot 2006, personal communication; Miller et al. 2006). Despite the importance of the species to global sea–air photochemistry, however, dynamic three-dimensional simulations of the oceanic distribution are only beginning to appear. We have recently obtained preliminary global results in the context of a biogeochemical general circulation code (Elliott et al. 2006). This early modeling effort is refined here, with validation against kinetic and pattern studies conducted over the last decade or so in the open Pacific.

Insertion of CO is a subset of general efforts in which we are now engaged to simulate multiple climate relevant trace gases in the marine environment. Mechanism development typically occurs within the global Parallel Ocean Program, a component of the U.S. Community Climate System Model [Parallel Ocean Program (POP) inside Community Climate System Model (CCSM); Drake et al. 2005]. Geochemical driver quantities are obtained from a standard CCSM ecodynamics code based at the National Center for Atmospheric Research and multiple universities (Moore et al. 2002; Moore et al. 2004; Collins et al. 2006). In the carbon monoxide case detailed in situ studies of vertical diel cycling are available as a start point (Johnson and Bates 1996). Further, dual hemisphere surface mea-

surements have been reported and used to compute sea–air flux, along with latitudinally resolved production (Bates et al. 1995; Zafiriou et al. 2003). We restrict our analysis mainly to the Pacific basin here, due to the availability of these relatively recent and coherent datasets. Photochemistry of the carbon cycle may be significantly different for alternate oceans, and they are less well studied (Zafiriou et al. 2003). The general model building strategy is to design reasonable parameterizations for production during organic photolysis and loss via microbial consumption, and then to vary critical mechanism features while examining measurements.

Our text is organized to reflect the development sequence: 1) addition of a dissolved gas to the OGCM, 2) scenario development with quality control, and, finally, 3) sensitivity testing. The POP marine simulation system is first described, by way of computational and physical configuration but also as a tracer transport model. Parameterizations, grid geometry, initialization, and run lengths are all detailed. It is noted that in its capacity as the CCSM marine component, POP is now augmented with a standard routine for the representation of major element geocycling (Moore et al. 2002; Moore et al. 2004). The introduction of climate-relevant trace volatiles is next described with reference to CO (Elliott et al. 2006). Ecodynamic imports from the major element code are listed, encompassing those that are required for both baseline and parameter variation experiments. The test series is next elaborated. A set of replicate CO bins is introduced simultaneously within a single model version. The tracers are treated identically except with respect to a photolytic constant, and this is altered widely in any one run. Special sections deal in the subtleties of carbon monoxide production and removal. These include the uncertainty inherent in representing chromophoric dissolved organics (Nelson and Siegel 2002) along with poorly known taxonomy of the consuming microbes (Zafiriou et al. 2003).

In the results section samples from a baseline and several sensitivity studies are presented as north-to-south sections through the middle of the Pacific. Comprehensive ship track measurement data are superimposed (Bates et al. 1995). Areas of agreement include the zonal position of peaks attributable to equatorial and middle-latitude frontal ecosystems (Longhurst 1998; Moore et al. 2004). Discrepancies are documented along the entire basin periphery. It is noted that at lower latitudes they may derive from the lack of aging/bleaching of model organics, the oversimplicity of our microbial population dynamics, or some combination thereof. Seasonality for the carbon monoxide distribution is next examined tentatively at the global scale, and integrated budgets are offered that are in substantial accord with earlier such calculations.

2. The transport/geochemical framework

Both test and production runs have been conducted exclusively within a biogeochemically enhanced version of the general circulation model known as POP. The coding is z level and descends from Bryan–Cox–Semtner ancestry (Semtner 1986; Maltrud et al. 1998). POP was developed originally in Thinking Machines FORTRAN as a tool for finely resolved physical oceanography studies (Dukowicz et al. 1993). Gridding has been configured as fine as one-tenth of a degree in some global simulations (Maltrud and McClean 2005). Recent emphasis on software

engineering has led to substantial improvements in performance on either vector- or cache-based supercomputers (Jones et al. 2005). POP has become a standard OGCM component within the U.S. CCSM (Drake et al. 2005). As such it is now supplemented with geochemistry-oriented subroutines handling ideal age tracers, the cycling of surface volatiles, and ecodynamics. The latter coding simulates major element transformations within the multiple organism classes defined in Moore et al. (Moore et al 2002; Moore et al. 2004). Nitrogen, phosphorus, silicon, iron, and light limitations all operate on the carbon cycle in these subprograms.

Since our goal here is the introduction of a completely new reaction scheme, we have opted to work within a relatively coarse POP model in order to maximize computational turnover. A grid that will be denoted as the "x3" underlies all carbon monoxide runs conducted so far. It was originally designed for paleo-oceanographic studies, but the same mesh has most recently been adapted by Peacock et al. (Peacock et al. 2005) to chlorofluorocarbon (CFC) penetration. Longitudinal spacing is 3.6° at the equator. Latitude intervals in the Tropics are 1° expanding to just under 2° in temperate regions. Singularity in the Arctic Ocean is avoided by smoothly displacing the numerical pole into Greenland. The Southern Ocean maintains a standard Mercator mesh all the way to Antarctica. Average cell size is about 3° on a side in x3 POP. In the vertical the model contains 25 nonuniformly divided levels varying from 12-m thickness at the surface to 450 m in the abyss. A range of advection schemes is available, but in our CO studies a third-order upwind formulation was selected in the interest of preserving monotonicity. Coarseness of the mesh demands state-of-the-art treatment for subgrid-scale processing, including both horizontal and vertical eddy mixing. The Gent–McWilliams and K profile parameterizations (GM and KPP) are thus invoked continuously. Surface forcing is accomplished by monthly average fields including temperature, humidity, and wind speed input from a National Centers for Environmental Prediction (NCEP) reanalysis. All references and substantial further detail regarding physical aspects of the setup are elaborated in Peacock et al. (Peacock et al. 2005).

The x3 POP was initialized with Levitus mean annual temperature and salinity, then spun up for 500 yr in a physics-only mode. Overall ecodynamics, biogeochemistry, and photochemistry were implemented simultaneously at this point. A minimum time scale often cited for approach to the upper-ocean biotic steady state is 3 yr (Sarmiento et al. 1993; Moore et al. 2002; Chu et al. 2003). Results reported here are extracted from no earlier than the third full annual cycle. Although carbon monoxide is controlled within the water column by short-lived entities, such as labile organics, these in turn may be influenced by large-scale geocycles. Following Moore et al. (Moore et al. 2004), we extended some of our simulations to three decades on a spot check basis.

3. CO in a trace gas module

POP is now an integral component of CCSM and is intended to function as Earth system model coding, so that a suite of climate-relevant trace gases can be introduced. Modular subprograms (Elliott et al. 2006) that import a subset of the Moore et al. (Moore et al. 2002; Moore et al. 2004) major element reservoirs and then adopt the concentrations and fluxes to determine local kinetics have been

standardized and documented. Mechanisms have been developed for dimethyl sulfide (DMS) and a variety of other volatile species (e.g., Chu et al. 2003; Elliott et al. 2006). Although DMS possesses a minor photolytic removal channel, this was nominally computed in proportion to photosynthetically available radiation (PAR) taken from the ecology. Carbon monoxide represents our first true foray beyond the visible spectrum. Primary sourcing occurs via interaction of ultraviolet with the dissolved organic matter. Chlorophyll densities are retained in these experiments to permit a more thorough handling of UV attenuation. Autotrophic biomass and free nitrogen forms are pulled in because they can be used to parameterize heterotrophic bacterial densities. A summary of options and selections for importation into our CO specific gas module is provided in Table 1.

It is normally the case with regard to marine trace volatiles that both production and removal parameters are poorly known. As we have worked toward comprehension of lower concentration compounds, formal optimizations have sometimes been employed to determine preferred rate constants and other types of kinetic parameters (Kasibhatla et al. 2000; Elliott et al. 2006). However, inverse methods can be strongly hyperdimensional and thus are taxing of computational/analysis resources. A simpler technique has been adopted for the present work because CO distributions are broadly dictated by just two terms—photolytic production followed by microbial uptake. The form of the removal kinetics and its implied rate parameters were established first, in accord with seagoing measurements. Water column chromophore properties and apparent quantum yields were then enfolded into a photolytic constant, which was rendered adjustable. The initial tracer number inherited into POP from full ecology simulations is about 30 (Moore et al. 2004). Ten new biogeochemistry slots were added inside the gas module here, but all were assigned to represent CO. The replicate molecules were given identical

Table 1. A sample of driver variables available in CCSM major ecodynamics routines, with selections for CO importation and brief justifications. Names are close to those within the coding but are adapted somewhat to enhance readability. Phosphorus tracers are omitted in favor of their nitrogen counterparts. The carbonate/alkalinity system is only relevant as a product pool for oxidation and so has been excluded (Mopper and Kieber 2002). Also, compare the early Moore et al. works (Moore et al. 2002 vs Moore et al. 2004) for exposition of a transition from variable to fixed Redfield ratio, which eliminated several species.

Tracer	Definition	Use	Explanation
no3	Nitrate	+	Parameterize bacterial densities in some runs
sio3	Silicate	–	
nh4	Ammonium	–	
fe	Dissolved iron	–	
doc(n,fe)	Dissolved organic C (N,Fe)	+	DOC as superset of chromophoric material
spC	Carbon as small phytoplankton	+	Parameterize bacterial densities in some runs
spChl	Chlorophyll as small phytoplankton	+	Attenuation of central wavelengths
spCaCO3	Calcite as small phytoplankton	–	
spFe	Iron as small phytoplankton	–	
diatC(Chl,Fe)	Carbon (Chl,Fe) as diatom	+	See small phytoplankton above
diazC(Chl,Fe)	Carbon (Chl,Fe) as diazotroph	+	See small phytoplankton above
zooC	Carbon as zooplankton	+	Grazing control on potential consumers

grid cell internal and sea–air interface removal, with the photolysis constant reset along the vector.

Starting with a central first guess derived from low-latitude diel cycling measurements, the photochemical proportionality was varied upward and downward in half-decadal increments. A best fit can be chosen via chi-by-eye or merit function analysis against ship tracks (Press et al. 1992). Additionally, improved parameter scales are definable for repeat runs. This process proved useful on several occasions, but in general we find it more practical to draw conclusions from the original settings. Results are presented in most of our figures as three curves representing surface concentrations from the initial central setting and immediate neighbors, presented in the latitudinal section. We have endeavored to emphasize lengthy cruise data extending fully in the north–south direction, so that a wide variety of ecogeographic provinces is sampled (Longhurst 1998). April and December data from the Bates et al. (Bates et al. 1995) collection address this need and also happen to be roughly phase offset in the sense of an annual cycle.

The built-in CCSM ecodynamics include all autotrophic classes contributing in the open ocean to primary production, along with an aggregate zooplankton bin and multielement detrital types. The major nutrient forms include nitrate and ammonia, silicate, and a single dissolved iron species. Early low-dimensionality tests of the x3 ecology model were spun up successfully over three years and provided realistic reproductions of oceanographic station data (Moore et al. 2002). More recently, runs have been extended to almost 30 yr and exhibit slight improvements in fidelity relative to satellite color measurements (Moore et al. 2004). We have been restricted here computationally to between 5 and 10 processors, residing on SGI Altix supercomputers at the Los Alamos and Oak Ridge National Laboratories. Given such resources 3-yr runs require several days on the wall clock so that many simulations were conducted over this period alone. Key scenarios amounting to about one-third of the total were extended to a full 30 yr. Most of the results displayed are from the third annual cycle, but differences from the decadal scale were mainly insignificant.

4. Production

Fundamental equations of aqueous photochemistry are outlined in early references such as Zepp and Cline (Zepp and Cline 1977) or Leifer (Leifer 1988) and are applied to carbon monoxide following the local modeling study of Kettle (Kettle 2000). By and large the Kettle symbols and nomenclature are repeated here, because they seem to be standard across the community (e.g., Nelson and Siegel 2002; Arrigo et al. 2003; Miller et al. 2006). Critical expressions are summarized in Table 2. Our approach is tailored for initial insertion into current-generation Earth system models and hence is very streamlined. In both the real atmosphere and ocean, far ultraviolet wavelengths are attenuated rapidly. Conversely, net or apparent CO yields fall with increasing wavelength in all reports to date (Zafiriou et al. 2003). In several spectral integrations the majority of photogeneration occurs in the traditional UVA bin, defined to be the range from 320 to 400 nm. In the present work a broadband approach is thus adopted, with averaging across these wavelengths.

While quantities in the table equations are all necessary in the comprehension of

Table 2. Summary of photochemical manipulations, with a reduction to the source terms incorporated into POP. Our approach derives mainly from the detailed local simulation of Kettle (Kettle 2000). The symbol θ indicates light angle after accounting for refraction, λ is a wavelength, *K* the diffuse attenuation coefficient, subscript *d* the net downward direction, ϕ an apparent quantum yield, *f* the fractional absorption attributable to organic chromophores, subscript *i* the list of major attenuating materials including CDOM, parameter *j* the photolysis proportionality estimated for the model, UVA the average energy from 320 to 400 nm, *k* an absorption per unit concentration, and bkgd a background attenuation usually negligible at short λ, with all other definitions provided in text. It is assumed that *E* may be expressed in Einsteins (Leifer 1988).

Equation	Explanation
$dE_d(\theta, \lambda, z)/dz = -K_d(\lambda, z)E_d(\theta, \lambda, z)$	Depth dependence of downwelling irradiance
Production $= \phi(\lambda)f(\lambda)K_d(\lambda, z)E_d(\lambda, z)$	CO input as a portion of energy deposition
$K_d(\lambda, z) = \Sigma a_i/(\theta$ factor)	Net for all species with angle adjustment
Production(POP) $= j$(DOM)(UVA)	Distilled to first-order photolytic form
UVA(z) $=$ UVA(0)$e^{-[k(\mathrm{DOM})+\mathrm{bkgd}]z}$	e-folding related to labile dissolved organics
k treated bimodally	Values are 0.003 and 0.01 (1/mμM)

upper-ocean photochemical processes, many are notoriously difficult to characterize. The downwelling attenuation coefficient, for example, is dominated by absorption of the chromophoric dissolved organic matter (CDOM) in the carbon monoxide case. But the beam coefficient a_g varies widely with depth, season, water mass history, and in studies even from a single laboratory (Nelson and Siegel 2002). The very chemical nature of remote oceanic CDOM remains controversial, for at least a significant portion of its mass (Benner 2002). Methods for the measurement of ultraviolet fluxes are still under refinement (F. Chavez 2006, personal communication). Given these difficulties, our strategy as modelers has been to collapse all photochemical terms into a compact expression of low molecularity. The proportion j is treated as a variable parameter with a first-guess value determined by actual surface ocean concentration trends. It is then altered in half-decadal increments to fill the replicate slots placed into the trace gas module during each run. Inspection of the Table 2 expressions reveals that j enfolds a variety of optical and photochemical quantities including the fraction of absorbing moieties within the organic content, chromophore target cross sections, and true microscopic quantum yields. All will vary with chemical and bleaching trajectories. Nonetheless, they are handled in the present model as large-scale averages.

Since we are aiming ultimately at dynamic simulation, the concentration of light-interacting entities must be derived at least implicitly from substances simulated in the major element routines. Moore et al. (Moore et al. 2002; Moore et al. 2004) carry a brand of dissolved organic matter (DOM), which they characterize as semilabile. Detailed distributions are presented in these references, and our simulations reproduce the results closely. Within the Moore ecology organics are given a brief, order-10-day time constant for remineralization. Refractory forms are therefore ignored within the standard CCSM biogeochemistry. The high levels of aged material known to accumulate in stratified regions are not captured in this approach. We make the approximation that modeled organics encompass most of the fresh material containing chromophores, which appears to decay dramatically

moving into the central gyres (Nelson and Siegel 2002). Furthermore, since any compensating effects internal to j are dismissed, the basin average fraction of absorbers is conceived of as constant. A round median concentration for dissolved organics in the surface sea is 10 μM in the Moore et al. simulations, and the value falls central to many reported measurements (Carlson et al. 1994; Carlson and Ducklow 1995). In the remote Pacific, a 10 contour follows boundaries for the northern and southern gyre ecological provinces and skirts the warm pool (Longhurst 1998).

Only a handful of in situ studies of mixed layer diel cycling have been reported for carbon monoxide in the open ocean. The most detailed Pacific data are tropical (Johnson and Bates 1996). Associated midday UVA intensities are reconstructed here from wavelength-dependent surface measurements made at equatorial and 20° latitude sites. The value obtained is 30 W m^{-2}. Daily averages were computed assuming a clipped sine wave of irradiance extending from sunrise to sunset. The result was compared with earlier tabulations for long-term, clear-sky conditions (e.g., Leifer 1988) by applying a minor cloud adjustment (Zafiriou et al. 2003). Our figure lies on the low side, but an intention during initial stages of the photochemistry modeling has been to retain round values as estimates wherever possible. Afternoon surface generation of CO averages 3 nM day^{-1} in the open, low-latitude regime. The median DOM line defined just above passed between major station locations (Tahiti versus the equatorial divergence; Johnson and Bates 1996). A reference j of 10^{-5} 1/d (W m^{-2}) may thus be established. It is identified as a central dashed curve in the upcoming graphics.

Biogeochemistry and trace gas routines operating under POP import monthly average shortwave radiation directly from physics driving the general circulation. Note that for the moment this means diel cycles of energy and mixing are smoothed together. Several one-dimensional studies of upper-ocean photochemistry show that there can be significant couplings (Doney et al. 1995; Kettle 2000). In a systems simulation mode, however, it is vital to link quickly with core planetary fluxes. Total incoming solar is converted to PAR in the CCSM ecology through the traditional fraction of 0.45 (Parsons and Takahashi 1973; Moore et al. 2004). Inspection of standard OGCM output with validation against textbook treatments (Piexoto and Oort 1992) indicates that about 100 W m^{-2} reach the ocean surface under typical low-latitude conditions. For the purposes here the approximation is made that a quantity 10% as large enters over the ultraviolet interval. The relationships are crude but form a convenient starting point for our photochemistry modeling. They are fully consistent with results from the driver depth profile studies we rely on (Johnson and Bates 1996). Carbon monoxide–relevant UVA is thus computed as 0.1 of PAR.

A simple expedient was adopted in order to extend the production calculations geographically. Wavelength and latitude-dependent surface energy inputs have often been provided, based upon analytical expressions for atmospheric attenuation due to ozone/aerosol effects or later relying on satellite instruments (e.g., Zepp and Cline 1977; Leifer 1988; Kettle 2000; Arrigo et al. 2003). Our calculations are verified against such data and in particular via relative results from the Leifer monograph (Leifer 1988), but they hinge on the measured tropical radiation field. We have informally integrated adjustments associated with transition to higher latitude, and to seasons of extreme solar angle. The factor of 10 scaling against

PAR is reduced where necessary, and it was found that increases could be ignored. A handful of tests was conducted early in the development process to address uncertainties such as the spectral dependence of cloud factors. Sensitivity was small and the results will not be reported. Improved handling of the time and location dependence of ultraviolet flux is definitely a priority. But we elect to defer the effort until a close connection can be made with atmospheric subprograms inside CCSM.

Attenuation as a function of depth is handled in a manner consistent with recent treatments of general aqueous photochemistry or biology (Sikorski and Zika 1993; Kettle 2000; Van Hobe et al. 2003; Arrigo et al. 2003). Ultraviolet incoming from the atmosphere is divided conceptually into two components, one direct and the other diffuse but emanating from the total sky as a luminous hemisphere of uniform brightness. The latter increases as the sun lowers toward the horizon, whether in a diurnal or seasonal cycle. Net angles of entry are within a few tens of degrees of vertical, and reflection is thus small. Refraction pulls the downwelling field even closer to the vertical. The effective pathlength through POP model layers is calculated as validation, given a range of angle factors. In practice the increase is considered to be encompassed in the overall uncertainty of scale depth. Although multiple sensitivity tests were conducted to investigate the effect, the runs reported here assume direct vertical propagation.

Assignment of the value K_d is particularly problematic. It contains a sum of absorption types but in the UVA and B regions CDOM tends to dominate. We compute downward attenuation from organic and chlorophyll contributions because they are readily available in the main biogeochemical simulator. All other modes of absorption are thus omitted. The approximation is probably safe over much of the globe, and we feel that it constitutes a reasonable startup approach. Measurements of dissolved organic absorption have been divergent among research groups. Nelson and Siegel (Nelson and Siegel 2002) present a critical review of the technical difficulties involved. We elect once again here to base our primary calculations on the in situ evidence. In the central Pacific in the vicinity of our 10-μM DOM median, scale depths for the downwelling field appear to be on the order of 30 m on average (Johnson and Bates 1996). The value a_g or a_{cdom} is formulated as k(DOM) with a k of 0.003 1/mμM. This arrangement is in accord with multiple season and depth-dependent determinations made at major oceanographic stations, and also with satellite color inversions (Nelson and Siegel 2002). The e-folding determinations performed during recent carbon monoxide budget exercises have been somewhat shorter but are astonishingly uniform over large regions (Zafiriou et al. 2003). It is not clear at this point whether the evenness is due to a sparse sampling protocol relative to fluctuations in the real optical field or perhaps to changes induced during handling. We treat the more rapid attenuation as our first line sensitivity test, resetting k to 0.01 to produce 10-m falloff at the semilabile median.

The production field configured in this manner is tailored uniquely to the needs of a particular systems model of ocean biogeochemistry, that of the Parallel Ocean Program carrying Moore et al. (Moore et al. 2004) major element cycling. The approach is clearly approximate at many levels. We fully intend to upgrade in the areas listed above as further expertise is acquired in the simulation of global ocean photochemistry. Research priority will probably be placed upon spectral resolution

and linkage to atmospheric attenuation. Despite the many inadequacies, however, it is maintained that our simulations have considerable pedagogical value.

5. Removal

Many investigators argue that the primary removal for carbon monoxide within the water column must be microbial (e.g., Johnson and Bates 1996; Zafiriou et al. 2003; and references therein). The case is convincing, although evidence collected thus far is partly circumstantial and a process of elimination often figures into the logic (Johnson and Bates 1996). Antibiotic introductions slow the oxidation reaction and known taxa can be identified in the laboratory as consumers. But beyond the basic assertion that bacteria are complicit, the mechanism is ill defined. We present a quick review of the situation to provide the reader with a flavor for the complexities that must be dealt with.

The organisms responsible for CO uptake in the open sea remain poorly characterized. They may be nitrifiers with the ability to derive energy from other small inorganics (Jones and Morita 1984a; Jones and Morita 1984b). Since removal is observed in the sunlit zone where ammonium oxidation tends to be suppressed (Moore et al. 2002), another possibility is that chemoautotrophic specialists are involved that resemble the nitrifiers. Bacterial kinetics are often modeled at the basin scale in Michaelis Menten form (Sarmiento et al. 1993; Christian and Anderson 2002). Most carbon monoxide analyses to date assume first-order behavior (Jones and Morita 1984a; Jones and Morita 1984b; Johnson and Bates 1996; Zafiriou et al. 2003), relevant below the saturation regime. Some authors maintain that radiocarbon introductions and unperturbed incubations give matching results, while others point to an enzyme-like saturation that reduces rates in the former case (Mopper and Kieber 2002; Zafiriou et al. 2003). Speedup of the oxidation occurs under shade, and this may be associated with a relaxation of light inhibition. Regionally resolved shipboard studies are sparse but indicate a Q10 of 2 (Zafiriou et al. 2003). Johnson and Bates (Johnson and Bates 1996) document for parallel sounding sites a significant slowing in more productive waters. They attribute the difference to variation in ecosystem structure.

Time constants reported for the microbial uptake are widely scattered, ranging at least from 1 to 1000 h over all remote waters (Kettle 2000), from 1 to 10 days based upon recent shipboard incubations but weighted at the lower end of the range (Zafiriou et al. 2003), and over a very similar spread when concentrations are monitored in situ but averaging about 3 days (Johnson and Bates 1996). As a starting point in the present work, we adopt the latter as representative for the Tropics. In situ methods depend for their accuracy almost exclusively on the ability of experimentalists to characterize local CO. Further, the value constitutes a round figure lying midway through the modern range. We feel that for the moment, ship-based and laboratory rates are best viewed as guides to actual water column removal. The potential for bias to be introduced during/after sampling remains high, through saturation, light, and filtration effects.

Detailed synthesis of the information relating to CO loss is currently lacking. For organizational purposes here we will divide marine bacteria into two broad classes with respect to interaction with the molecule. Heterotrophic generalists are the major recyclers in remote areas and subsist mainly on bulk dissolved organics.

Moore et al. (Moore et al. 2002; Moore et al. 2004) ignore the heterotrophs in favor of a Q10 remineralization rate for DOM. In our work on dimethyl sulfide we have on occasion parameterized the generalizing microbes as log linear with respect to phytoplanktonic nitrogen (Chu et al. 2003; Elliott et al. 2006). The relation to biomass is known to be rather weak (Carlson et al. 1996), and independence is reflected in simulations of both large-scale distributions (Fasham et al. 1993) and DOM processing (Christian and Anderson 2002). We place organisms such as the nitrifiers or their analogs into a second category here. Energy for chemically driven fixation may derive from a stream of small reduced molecules including ammonia, the monoxide, or both. On the removal side, such populations are likely controlled by microzooplankton. Small grazers have access to other food and in particular the heterotrophic biomass. Their densities are reflected in measured and perhaps even modeled aggregates. There would seem to be the opportunity for consumer pressure to influence at least some portion of the CO geocycling rate.

With this overview in mind, we now select several loss forms for testing. A baseline is defined in the interest of parsimony as the average applied at all locations $-\mathrm{CO}/\tau$, where τ is 3 days. Clearly, this is only a crude approximation, but it provides a surprisingly faithful reproduction of real patterns. Refinements posed as sensitivity tests are summarized in Table 3. Ten-degree doubling is in accord with reduced rates observed in the Southern Ocean (Zafiriou et al. 2003). The possibility that slow removal may be connected with biological activity is addressed first as a parameterization against nitrate. Active bacterial populations may require a period of the order of several growth times to become established. As fresh material reaches the ocean surface, photolysis of DOM may well precede microbial interaction. Within our nitrate function, the lifetime is clamped on the fast side at a single day. This is consistent with both maxima obtained in situ (Johnson and Bates 1996) and the bulk of measurements from regionally distributed work (Zafiriou et al. 2003).

Table 3. Construction of removal terms. The baseline is a simple pseudo-first-order process assigned a global average rate constant. Q10 is a standard biological reference to rate reductions associated with enzyme kinetic temperature dependence. It refers to change per ten ambient degrees. Temperature is expressed in Celsius and is keyed to local conditions, not SST. *B* signifies a poorly defined nitrifier or analog. *P* is a generic production, with subscript *S* referring to the sum of small reduced substrates or the compound at hand. The *Z*s are some microscopic portion of the model aggregate zooplankton. Expressions containing *B* presume Michaelis Menten undersaturation. In the sea–air transfer line, PV signifies a Schmidt number–dependent piston velocity and *H* the Henry's law constant. Subscripts *l* and *g* denote the liquid and vapor phases.

Equation	Explanation
Internal removal = Q10(CO)/τ	Form for most runs
Q10 = 2.0**[(T − 30)/10]	Set to unity in baseline
τ = 1d or if nitrate >3 μM [1 + (no3 − 3)]	Time scale slows in upwelling regimes
Internal removal $\propto B$(CO)	First-order bacterial term
Substrate production $P_S \propto BS \propto ZB$	Nitrifier-type steady state, e.g., S = ammonium
$B \propto P_S/Z$	Microbes scale as inverse microzooplankton
Internal removal $\propto P_S$(CO)/Z	Substitute for B above
Surface loss = PV[$\mathrm{CO}_l - \mathrm{CO}_g/H(T, S)$]	Temperature and salt dependence

A more speculative notion is that grazing control explains a linkage of ecosystem primary production with reduced rates. Here we refer solely to the hypothetical nitrifier-like class. First-order kinetic dependence is inserted into the loss term (B in the table). Proportionalities are now provided as opposed to actual equations because we wish to emphasize functionality. In the B(CO) entry, the usual Michaelis Menten form is collapsed into the undersaturation regime. Half-maximum levels and rate constants have coalesced. Similar simplifications apply to the next few table lines as well, and they further constitute a steady-state analysis. The substrate S can represent ammonia, carbon monoxide, both together, or unspecified energy sources. Pressure will be exerted by the microzooplankton denoted by Z, so that B should depend inversely upon them. In our simulations microconsumers are assigned a constant, small fraction of zooC (Table 1). The form ultimately adopted in the model is then internal removal $= cP_S$(CO)/zooC, where c incorporates several implicit parameters and is adjusted to reproduce the global burden (Bates et al. 1995; Zafiriou et al. 2003). Two subclasses of this loss type were explored. The hypothetical specialist was supported first by an independent source (S = ammonium + other), and then by CO itself. In the former case we expect the trace gas to correlate both zooplankton and the inverse of substrate flux. In the latter, carbon monoxide sustains the entire sequence and its production cancels ($P_S = P_{\mathrm{CO}}$).

Ecosystem structural influences on the CO distribution are of interest because there is the potential to synthesize disparate removal data (Kettle 2000; Zafiriou et al. 2003). Several POP runs were therefore conducted with grazing included as in $B \propto P_S/Z$, but they should be considered merely suggestive. Metabolic and biophysical constraints enfolded in c have only been checked in a gross sense (Parsons and Takahashi 1973; Jumars 1993). They include the ratio of source molecules to net fixation, mass conservation limits on zooplanktonic carbon, and the microphysics of diffusion. Further, the computations rely in part on kinetic equilibrium. A more complete approach would involve separate bacterial population dynamics. Models of other marine gases and of the overall dissolved organics have adopted such an approach (Christian and Anderson 2002; Archer et al. 2004). Significant difficulties would be encountered in parameterization of saturation and preference constants, but critical uncertainties might be reduced in the attempt.

Transfer of carbon monoxide into the atmosphere is a subsidiary sink in most locations (Bates et al. 1995; Zafiriou et al. 2003). However, it is crucial to incorporate for at least two reasons. Losses to the gas phase are required to balance regional budgets, and surface fluxes will figure prominently in models of marine tropospheric oxidation. Sea-to-air transfer is included in our model for all surface grid points. The algorithm has been discussed in Elliott et al. (Elliott et al. 2006) but a condensation is merited here. Atmospheric momentum fluxes pass from POP into the trace gas module and are utilized there to set boundary layer wind speed profiles. Ice coverage transfers into the gas subroutines as well. Piston velocities are computed per Wanninkhof (Wanninkhof 1992). Schmidt numbers are derived from the laboratory measurements of Wise and Houghton (Wise and Houghton 1968), with salt adjustments as outlined in Bates et al. (Bates et al. 1995). Temperature-dependent Henry's law expressions trace to Wiesenburg and Guinasso (Wiesenburg and Guinasso 1979).

Within the lower atmosphere concentrations of carbon monoxide tend to lie at

mixing ratios of many tens of ppb. The molecule has both natural and anthropogenic combustion sources upon the continents (Crutzen and Zimmerman 1991; Kanakidou et al. 1999). The inputs can be quite strong and are reflected in a temperate maximum in the Northern Hemisphere. A gradient leads downward across the ITCZ to the relatively well mixed reservoir in the south. The oceanic photochemistry mechanism under development is currently configured in a standalone POP. We thus have the luxury of fixing lower-tropospheric CO distributions. The gas phase measurements of Bates et al. (Bates et al. 1995) are adopted for their coherence with surface ocean data. Latitudinal averages were constructed from multiple cruises.

6. Results

Our major surface seawater carbon monoxide computations have been prioritized for presentation as shown in Table 4. The full baseline scenario given in the first entry couples deeper penetration of ultraviolet radiation with the fixed biotic uptake time. Shoal attenuation maintaining the same removal rate was then investigated, followed by a return to the original propagation (30-m *e*-fold at our model DOM reference) but with Q10 adjustments. Last, the nitrate and zooplankton parameterizations of ecosystem structure are explored. Runs not mentioned in the table include *j* offsets relative to the central tropical calculation, experimentation with the number and width of radiation intervals, and cloud effects on the UVA distribution.

Relative to each run our analysis sequence begins with the longest north-to-south ship tracks. Specifically, we elect to focus on Pacific datasets with numerous surface concentration measurements cross cutting a maximum of ecological provinces. Examples are described in Bates et al. (Bates et al. 1995). Two cruises have proven especially useful for model comparison. They are labeled the Radiatively Important Trace Species campaigns of 1993 and 1994 (RITS93 and -94) in the original reports. Gulf of Alaska and extreme Southern Ocean samples are among the data, reflecting the biogeographical PSAG, SANT, and ANTA zones (Longhurst 1998). The two transects run along the same meridian (140°W) but are offset by almost six months and correspond to spring/fall in the respective hemispheres. Although there is evidence that the averaging processes implied in our mechanism led to difficulties at the basin periphery, a planetary-scale result is nevertheless presented tentatively to conclude.

Table 4. Organization for the CO runs. Within each simulation, *j* from Table 2 is treated as a parameter varying over half decades. Source term uncertainties are manipulated internally because they are currently more tractable. Sea–air transfer is fixed in the Wanninkhof (Wanninkhof 1992) form throughout.

Tag	Source configuration	Sink configuration
Baseline	$k = 0.003$ (1/mμM)	$\tau = 3$ days
Enhanced attenuation	$k = 0.01$ (1/mμM)	$\tau = 3$ days
Q10	$k = 0.003$ (1/mμM)	Q10 slowing
Growth phase	$k = 0.003$ (1/mμM)	Nitrate dependence
Grazing control	$k = 0.003$ (1/mμM)	τ proportional to (Z/P_S)

We begin in Figure 1 by superimposing year-3 results from the model over the 140°W data. The intermediate j value 10^{-5} 1/d (W m^{-2}) is associated with the central dashed profile. This and the succeeding curve with log(production) roughly 0.5 greater bracket the measurement averages at many latitudes. Our baseline run has several important features in common with the observations. The year-round peak near the equator is attributable to a combination of persistent photon fluxes with a new-nutrient-driven biota generating plentiful organics. Falloff is seen moving into the subtropical gyres in both cases. The model produces peaks or shoulders near 20° in either hemisphere, which are not apparent in the data. Similar features have been noted in earlier POP biogeochemistry and trace gas simulations (Chu et al. 2003; Moore et al. 2004). They are not fully understood but appear to be connected with sensitivities of the physical simulation along equatorial current system fronts (Tomczak and Godfrey 1994; Maltrud et al. 1998). Maxima in the vicinity of 40° north or south can be assigned to the midlatitude bloom zones (Parsons and Takahashi 1973; Longhurst 1998). In the North Pacific a strong decay is inferred passing through fall and into winter. As inputs of UVA recede, the monoxide seeks Henry's law equilibrium in colder waters. Saturation is a few tenths nanomolar computed relative to an atmospheric concentration of 100 ppb. The reductions are also suggested between 40° and 60°S but are less obvious because of the time phasing.

On the whole these areas of agreement may be viewed as encouraging, given the simplicity of the model. Concentration ratios from the Tropics to gyres to middle-latitude frontal systems appear to be reasonable. Timing of the seasonal cycle is reproduced, and in colder provinces there is an onset of gas–liquid equilibration during darkening periods. Average concentrations can be represented given a single first-order photolytic proportionality. An alternative position is that the concordance with data may be somewhat fortuitous, since the real ocean probably does not maintain anything resembling a fixed removal constant. But it will be seen below that variations in the loss form do not degrade model performance significantly.

Clearly, the dashed curve and its upper neighbor consistently provide under- and overprediction, respectively. A preferred value for j in the baseline is around 2×10^{-5} 1/d (W m^{-2}). It is momentarily advantageous to withhold resimulations using this figure because the optimum shifts in other situations. The configuration derived from surface observations produces low concentrations because local mixing effects were ignored. At the beginning of a diurnal cycle, water parcels circulate vertically. When they are near the interface, more than the average diurnal CO is acquired per unit time. The inputs propagate downward and even the depth profile. Since a systematic j variation is incorporated into every run, the answer most appropriate on an integrated basis may be calculated post hoc.

Evenness of the tropical profile accentuates our 20° shoulders, and depth dependencies again provide an explanation. The upper column turns over distributions of carbon monoxide and its semilabile precursors on almost a nightly basis (Kettle 2000). DOM is also distributed somewhat evenly through the mixed layer (Nelson and Siegel 2002). If the Table 2 UVA equation is averaged over z, the scale length $1/k$(DOM) emerges as a premultiplier, and cancellation of the dissolved organic concentration ensues. For example, equatorward of a 10-μM median the e-folding may be 10 m in areas where the top of the thermocline lies

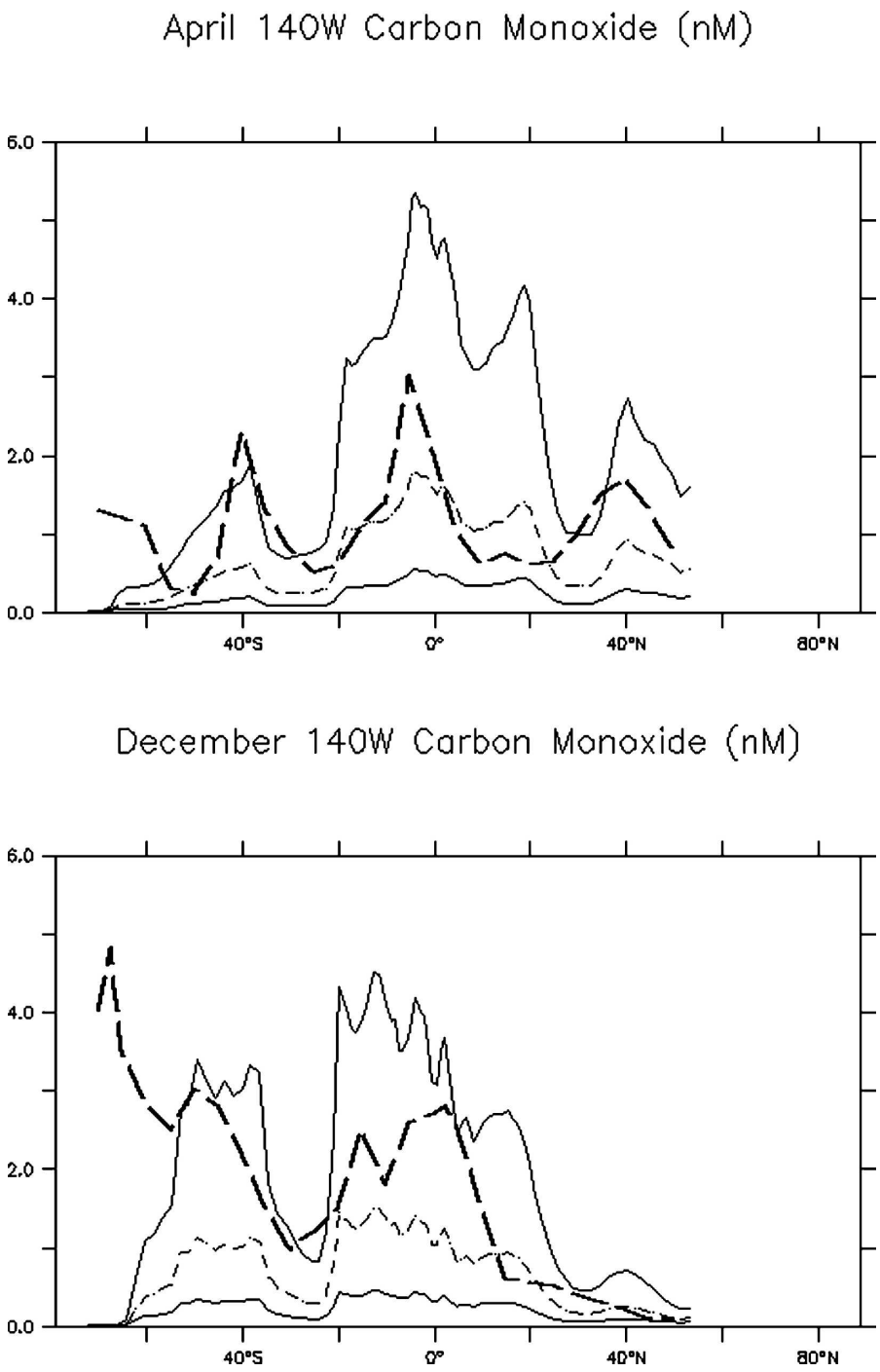

Figure 1. Sections taken from results of the Table 4 scenario labeled baseline, for locations aligned with long north–south ship tracks. The thin dashed curve is associated with a starting value for the photolytic constant *j* as defined in the text. Neighboring continuous contours differ in production rate by half a decade (3 or 0.3). Thick black dashes summarize the measurements (Bates et al. 1995).

several times deeper. All photons are effectively absorbed and column CO generation is dictated by the incoming energy. However, chromophore levels drop precipitously near borders with the oligotrophic regime (Nelson and Siegel 2002; Moore et al. 2004). There the downwelling photon stream goes mainly unattenuated. Proportionality with DOM is restored, and production tracks the organic concentration pattern.

There was concern entering into the CO project that portions of the polar ocean might not be fully biogeochemically equilibrated at the end of runs only 3 yr in duration. There had been difficulty with the evolution of dimethyl sulfide distributions in the coastal seas of Antarctica (Chu et al. 2003). Accordingly, 30-yr photochemical simulations were conducted here in some cases. Concentration distributions were examined over the entire globe every decade but with special attention paid to polar waters. The Table 4 baseline was among runs extended in this fashion. Deviations relative to the third model year were small—one-third nM or less. Rapid equilibrium is perhaps expected in the present instance, because surface waters communicating with the central ocean in high-latitude winter will also move toward Henry's law. Dissolution/removal steady state is reached in the top few tens of meters of the POP model within days. It is also true that the proximate source/sink entities DOM and the bacteria are short lived. However, some divergence documented between years 3 and 30 involved buildup along the tropical shoulder features. Accumulation of organic precursors may be implicated, taking place within the tropical thermocline.

The largest discrepancies against measurement occur at southern latitudes of between 60° and 70°. This is the most difficult aspect of our runs to assess. No attempt was made to moderate carbon monoxide removal rates in darkness. The model will thus drift during winter toward flux/removal balance. Eventually surface concentrations lie just below Henry's law. Sample times in the figure are not amenable to the evaluation of this bias, but even saturation concentrations would constitute gross underprediction. Furthermore, the problems are amplified as the sun returns in spring. The RITS93 and -94 expeditions took place during periods of steep decline in Antarctic stratospheric ozone. We estimate that an implied excess of UVB radiation can account for only a small portion of the deficit (Arrigo et al. 2003). Loss of upper-atmospheric attenuation may contribute in part, and this is a main reason spectral resolution must eventually be introduced. But stratospheric trends do not appear to be a dominant explanation.

It is of course tempting to invoke missing sources with regard to Figure 1. Limited evidence exists for dark reactions yielding CO at depth (Johnson and Bates 1996; Zafiriou et al. 2003), and the processes involved might come into play during polar night. Order tenths nanomolar have sometimes been measured below the euphotic zone. Buildup to similar levels is reported in isolated laboratory samples. The possibility of contamination could not be excluded in either case. Dark CO could in principle be handled by introducing a background generation sufficient to maintain low levels in the thermocline. Since time constants are normally set to several days, one-tenth nM day^{-1} might be sufficient to reproduce the putative data (e.g., Johnson and Bates 1996). Underestimates in the Southern Ocean lie within the realm of seasonal sea ice. POP routinely passes fractional surface coverage into the tracer module to restrict gas transfer. This would seal off the atmospheric source but permit increases underneath. One hundred days of

injection below ice could well make up the high-latitude concentration deficit, but the ultimate sources of energy and carbon would be poorly defined. We have elected here to omit dark inputs because they would be extremely speculative. Loss times estimated aboard ship are slow in the Southern Ocean during the production period (Zafiriou et al. 2003). This effect may explain a portion of the divergence, but Q10 simulations to be described suggest that it is not by itself sufficient.

Results from the extra-baseline runs of Table 4 are instructive both due to differences and similarities with the above. Sections along the 140°W meridian are offered in Figure 2 for the shoal penetration experiment. Per unit j, tropical concentrations are reduced significantly. The DOM cancellation tendency leaves surface UV and effective yield as dominant factors in the determination of production. The former is computed independently, but efficiency is suppressed implicitly within j as absorption rises. An equivalent argument is that column-integrated energy deposition is simply reduced within the term j(DOM)(UVA). Gyre concentration patterns remain unchanged. Ultraviolet wavelengths go unattenuated in this regime. Given a conjunction of low-latitude reductions with oligotrophic constancy, the value 3×10^{-5} 1/d (W m^{-2}) is optimal. Strengthened absorption softens the surface profile in this section. Unfortunately, the equatorial peak is lost for several months and the band of high concentrations in southern temperate waters narrows conspicuously. A shallow light penetration mechanism is currently viable and cannot be excluded from our list of candidates, but it is not a parsimonious option.

Altered removal scenarios fall in much the same category. Figure 3 provides results from the Q10 adjustment. As anticipated, tropical contours are mainly unaffected. Small equatorial increases derive from the reference temperature choice—upwelling waters tend to be cooler but 30° is standard (Parsons and Takahashi 1973; Moore et al. 2002). The prominent effect in model sections is uplift of the polar wings. Although temperature spans nearly three decades centigrade over the domain, concentrations do not increase by the factor 2^3 because sea–air transfer provides a kinetic cap. In profile the changes resemble those for enhanced attenuation, but j is displaced in the opposite direction. Since losses are depressed, production need not be as intense. Modest improvement may be noted near 60°S, but the gains do not continue poleward. This may once more point to an omission of mechanism channels. Introduction of the nitrate-dependent lifetime is more intriguing. Output slices are offered in Figure 4. The time constant was clamped in low nitrate areas at the round figure one day. The value is consistent with much of the rate distribution acquired during recent shipboard measurements (Zafiriou et al. 2003). Carbon monoxide concentrations drop in oligotrophic waters in response to the fast processing, and the equatorial peak stretches a bit since upwelling nitrate can rise above the 5-μM level corresponding to our previous fixed lifetime. Tropical shoulders are smoothed in the 20° vicinity. Gyre dips are accentuated excessively, but the qualitative feel of the ship tracks is preserved. This suggests that the ecosystem structure concepts expressed by Johnson and Bates (Johnson and Bates 1996) have merit—removal may be faster in impoverished waters.

Microbial kinetics of carbon monoxide uptake are probably quite complex in the real ocean. They should involve at least the following steps: 1) preference weighted growth upon several food items, 2) grazing terms with the microzoo-

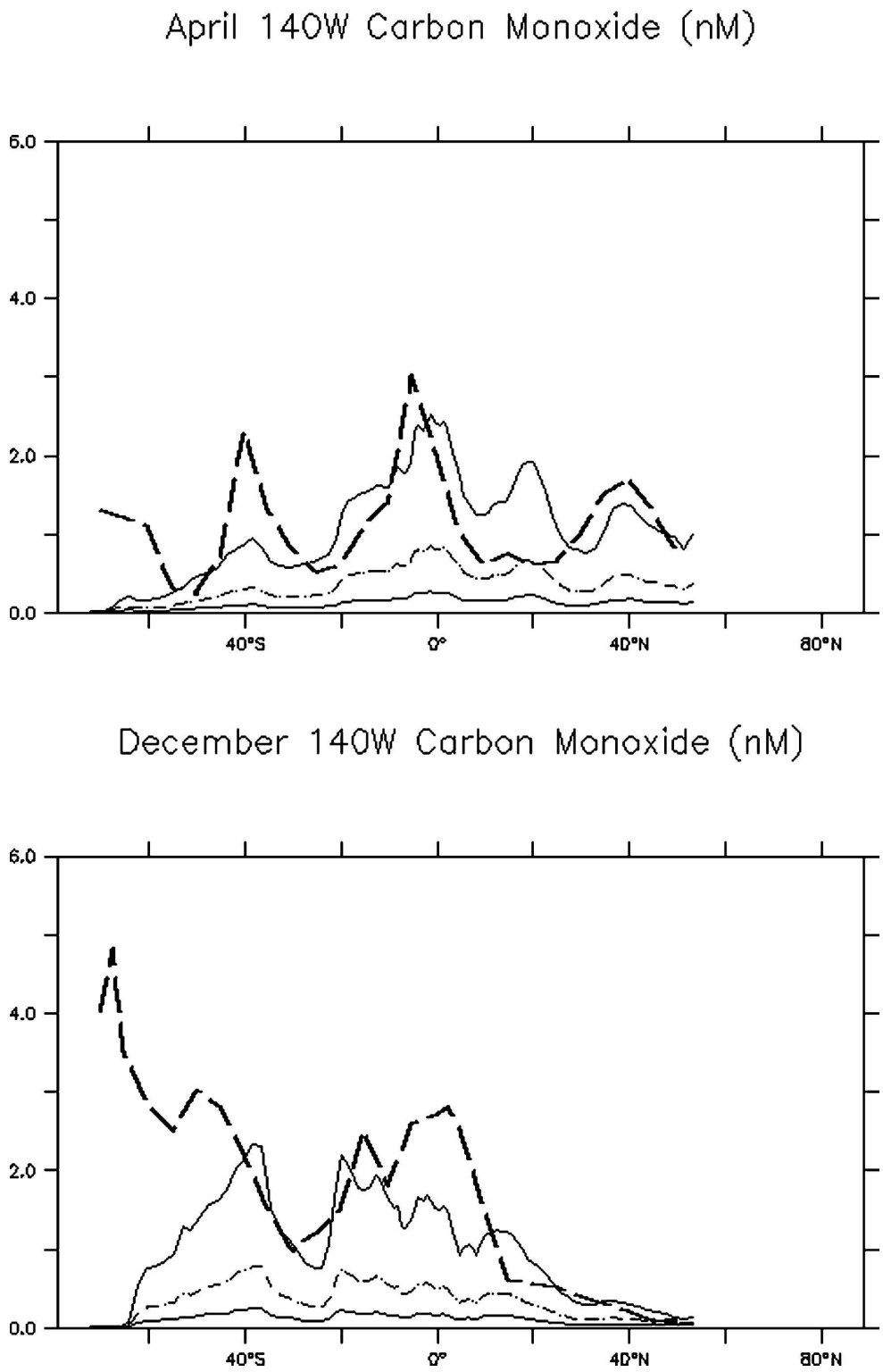

Figure 2. Same as in Figure 1, but for the Table 4 scenario labeled enhanced attenuation.

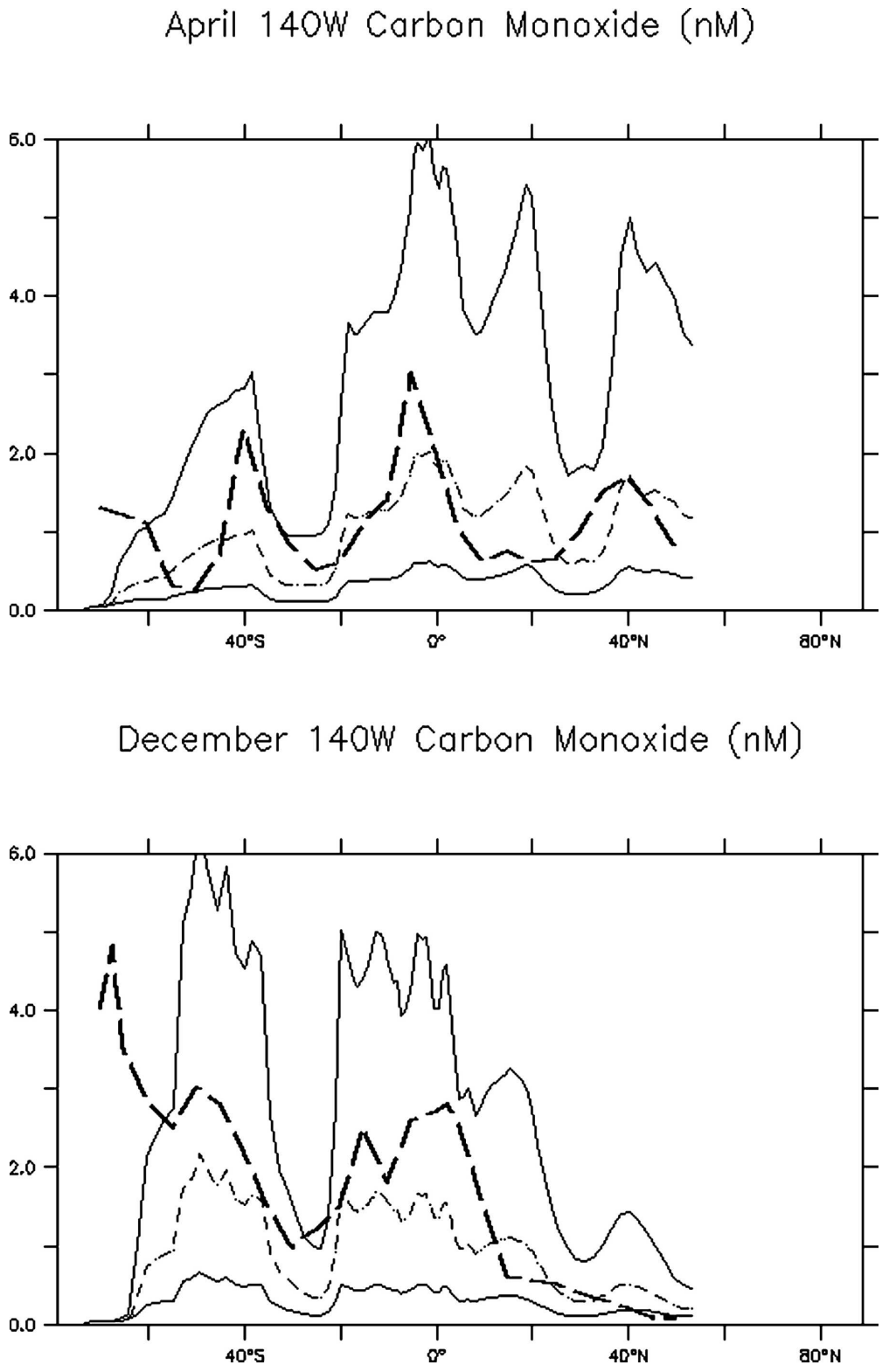

Figure 3. Same as in Figure 1, but for the Table 4 scenario labeled Q10.

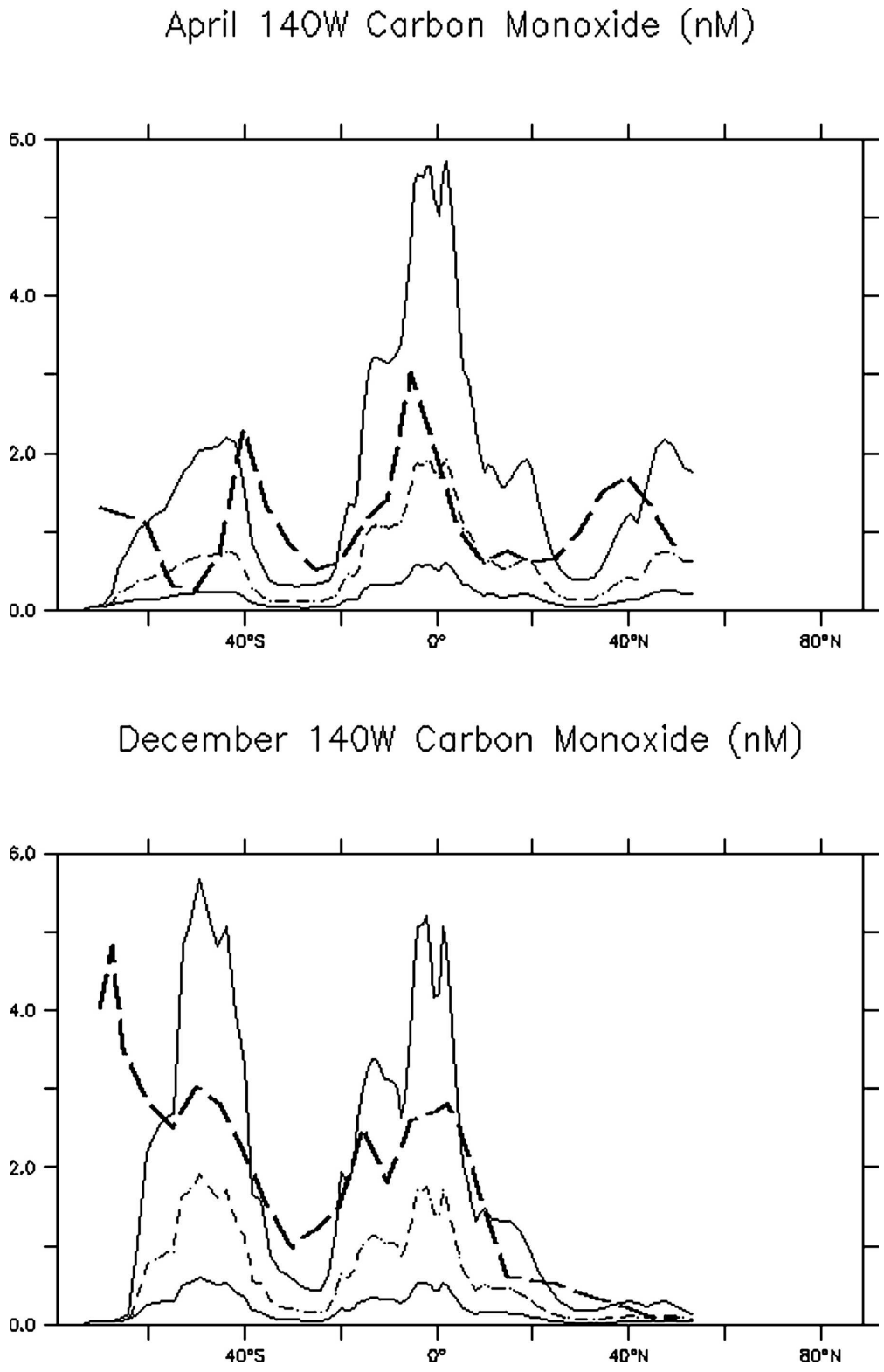

Figure 4. Same as in Figure 1, but for the Table 4 scenario labeled growth phase.

plankton subsisting on smaller organisms, and 3) consumption extending on to higher trophic levels. This sequence is embodied in our Table 3 mechanism in a highly simplified manner, as an undersaturation steady state. Data regarding CO remain quite scarce, and it has been our judgment that a detailed treatment is not yet warranted. However, the information that is available points strongly to bacterial behavior as a key to comprehension. Two special cases were identified above in the removal section, with carbon monoxide controlled by microbes lying along an alternate substrate line or else one dependent upon the molecule itself. Appropriate lifetime expressions were inserted into several model runs, with the realism of aggregate parameters such as growth rates, metabolic factors, and diffusion control verified in retrospect.

Patterns implied in the mechanism table for a generic substrate flow P_S were studied first. Results had the direction and magnitude predicted earlier (CO $\propto Z/P$). Recall that if the support compound S is the monoxide itself, coincidence within the kinetic equilibria ($P_S = P_{\mathrm{CO}}$) translates to a strong link with grazer densities and sacrifice in the dependence upon absolute production. Under these conditions the B(CO)-type removal produced a systematic collapse in profile spread. The phenomenon is so stark that figures generated in the manner of 1 to 4 prove difficult to read if they refer to more than a handful of js. As a concise surrogate we have calculated the ratios of local concentrations, among 10 replicates for one run in which the Table 3 substrate was presumed to be CO. Successive concentrations were divided by values from preceding j curves, sampling every 10° of latitude over the April and December locations. The quotients averaged 1.4 with a deviation of 0.4 and this outcome was typical. Contours were simply packed together, in a rapidly repeating and highly condensed group. Clearly, in some of our grazing control simulations, dependence on the carbon monoxide production is severely diminished. Proportionality to the imported Moore et al. zooC in fact becomes dominant. All this can be accomplished within POP given realistic zooplanktonic growth rates of the order of unity per day (Jumars 1993), with implied half-saturation levels matching those for known small molecular energy sources (Sarmiento et al. 1993; Moore et al. 2002) and a fractional microscopic component Z approaching 1%. We suspect that population dynamics of consumer bacteria and the extent to which they behave chemotrophically may ultimately prove crucial to completing the photochemistry simulations.

Results from the periphery of the Pacific basin force us to temper many of our conclusions. Refer, for example, to Figures 5 and 6, in which baseline sections are offered for alternate longitudes and shorter cruises (Bates et al. 1995). Near the international date line dashed and upper plots once again do a reasonable job of bracketing the measurements. At 100°W, however, reduced j values give a superior fit at the equatorial upwelling. One might postulate that dissolved organics in this area are sufficiently fresh that their chromophore content is underdeveloped. Since aging and bleaching are more usual explanations for this behavior (Nelson and Siegel 2002), the explanation is unsatisfying. Heightened bacterial activity could be cited, but we have already been at pains to argue that productive waters consume the monoxide slowly. The Moore et al. (Moore et al. 2002) model may bias the DOM field, but data are lacking so that this possibility is difficult to check. In the vicinity of Micronesia in Figure 6, even central model contours are uniformly high. Here in the warm pool organic aging is perhaps expected, but deco-

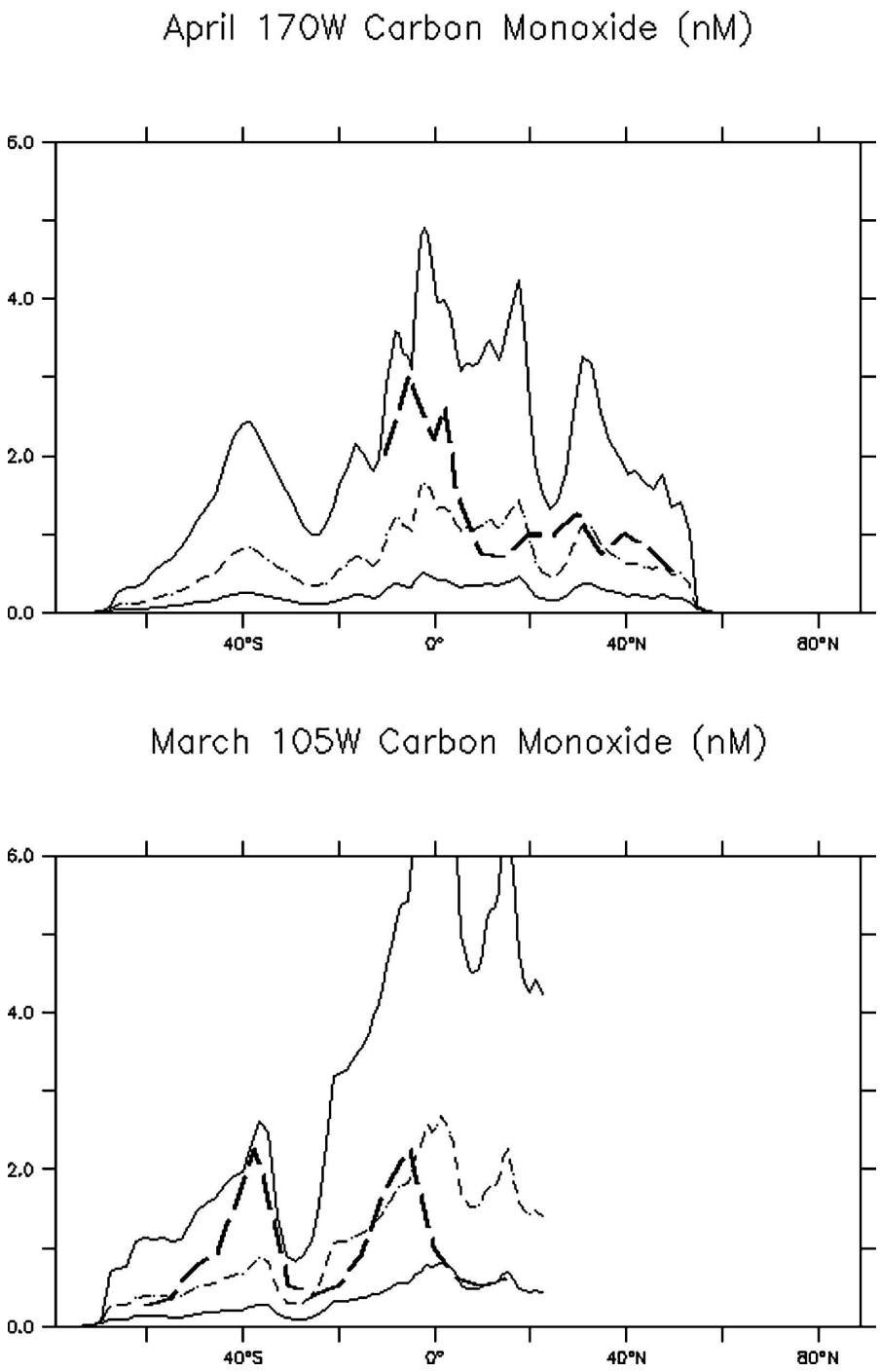

Figure 5. Sections taken from shorter track measurements, along with the related baseline calculations. (top) Near date line and (bottom) the eastern basin. The thin dashed curve is associated with a starting value for the photolytic constant *j* as defined in the text. Neighboring continuous contours differ in production rate by half a decade (3 or 0.3). Thick black dashes summarize the measurements (Bates et al. 1995).

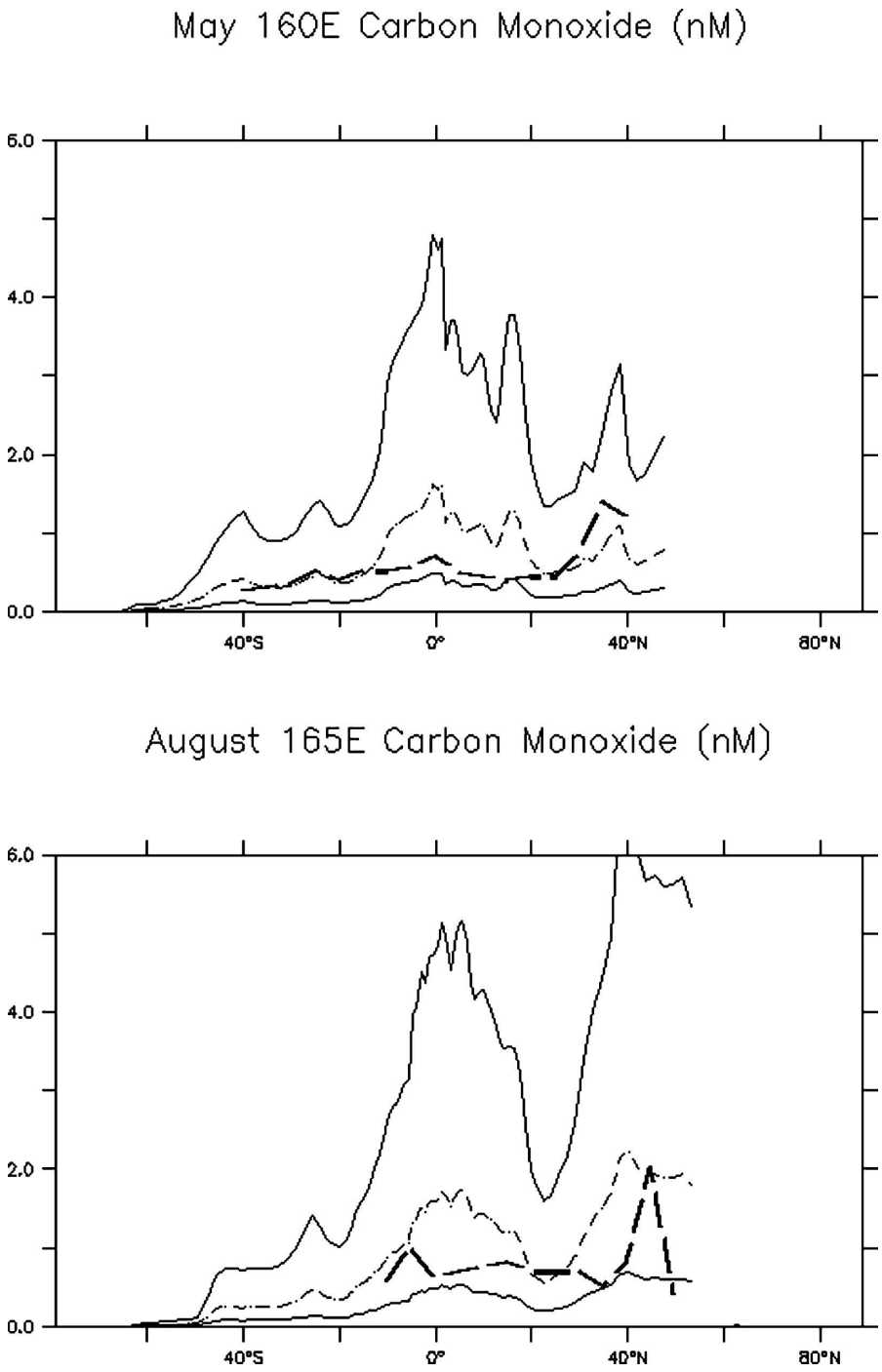

Figure 6. Sections taken from shorter track measurements, along with the related baseline calculations. Results here are from the Asian side of the Pacific. The thin dashed curve is associated with a starting value for the photolytic constant *j* as defined in the text. Neighboring continuous contours differ in production rate by half a decade (3 or 0.3). Thick black dashes summarize the measurements (Bates et al. 1995).

herence with the opposite side of the basin is disconcerting. An underlying message may be that dynamic treatment will be required for each of the quantities' DOM, its light interacting component, and the CO specific bacteria.

The baseline, Q10, and 10-m simulations offered here all appear relatively creditable. As we move into coupled upper ocean–tropospheric photochemistry experiments, the tendency is to begin with base or temperature-dependent mechanisms because they are streamlined. Ship track references are limited here to the longitude range 150°E to 100°W. Most laboratory and kinetic data cited come from this sector as well. There are several reasons to believe that geochemical cycling of carbon monoxide will differ in the Atlantic. The Aeolian iron flux is significantly higher there (Moore et al. 2004), plus riverine inputs are focused so that terrestrial DOM is favored (Zafiriou et al. 2003). These issues await later attention, but we feel that at a preliminary level, our model may be extensible to the total ocean. Figure 7 thus provides a sample of global-scale results. To generate the plots our baseline was rerun at the j setting 2×10^{-5} 1/d (W m^{-2}). The most obvious seasonal effect is a swing toward high CO following the path of the sun. Intense photon inputs lead to a strong flow of carbon monoxide out of surface

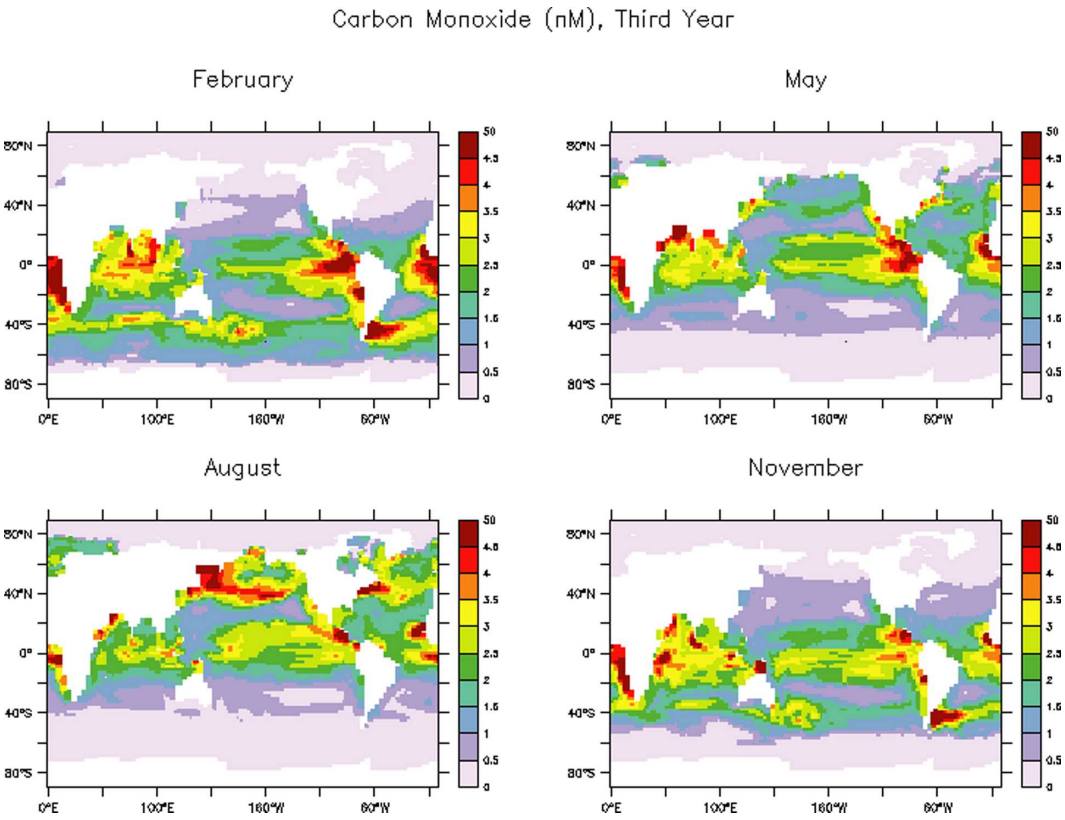

Figure 7. Global carbon monoxide concentration distributions simulated in the baseline scenario during the third model year, given the photolytic constant 2×10^{-5} 1/d (W m^{-2}). Averages were taken from central months in each of the four seasons.

seawater. Decay toward the gas–liquid saturation level of the order of tenths nanomolar (Bates et al. 1995) is apparent during dark periods. Scattered maxima associated with tropical and eastern basin upwellings may have predictive value and merit investigation.

Large-scale budget exercises have recently been reviewed for CO (Zafiriou et al. 2003), and it is useful to compare with current results. Since we aim intentionally at the Bates et al. (Bates et al. 1995) measurements and compromise on 3-day removal, the outcome is determined a priori in part. We have integrated concentrations and rates for the entire domain over the third year of the baseline simulation shown in Figure 7. The mixed layer averages 1.4 nM. Pacific Marine Environmental Laboratory (PMEL) datasets produce a value very close to unity overall. Removal during year 3 totaled 35 Tg carbon as CO. The Bates results imply 25 Tg if they are taken to be the average for a 50-m mixed layer. The present work not only begins from a slightly higher level but is three-dimensional so that it accounts for tailing into the thermocline. Zafiriou et al. (Zafiriou et al. 2003) adopt methods that are coarsely resolved but otherwise comparable. These authors derive rates of 30–50 Tg C–CO per year based on somewhat faster lifetimes. Within a few years in all simulations, POP losses are closely in balance with production. In unpublished results, Fichot et al. map out the inputs based on an inversion of remotely sensed absorption. The distributions are broadly consistent (C. Fichot 2006, personal communication; Miller et al. 2006). Sea–air transfer of the monoxide integrates to 6 Tg C–CO per year in the figure, only slightly higher than estimates based on cruises (Bates et al. 1995). Relative convergence of the flux estimates may be attributable to systematic underprediction at windy latitudes.

Collective areas of agreement between our model and earlier analyses are noteworthy given the divergence of treatments. Carbon monoxide budgets for the ocean surface were for many years quite scattered (Logan et al. 1981; Erickson and Taylor 1992; Zafiriou et al. 2003). The similarity cited here indicates that comprehension of the geocycling is stabilizing. But the tale is also cautionary. We expect that in the future there will be a need for more careful cross comparisons. Yields and absorptions must be reconciled with one another. Multiple production paths probably exist and should be parameterized such that global change influences are represented. Similar statements could be made regarding the microbial uptake.

7. Summary and discussion

The small, photochemically active compound carbon monoxide lyses from marine dissolved organic matter under the influence of ultraviolet radiation. Its production constitutes a major channel in the ocean carbon cycle (Kettle 2000; Mopper and Kieber 2002). Crossing into the troposphere because it is volatile, the molecule exerts control on gas phase oxidant distributions (Logan et al. 1981; Crutzen and Zimmerman 1991; Erickson and Taylor 1992). Feedbacks are implied on removal times for both direct and indirect greenhouse species (Houghton et al. 1996). Taken together these points indicate a need to include CO in Earth system models. We are therefore developing large-scale parameterizations for the associated mixed layer processing. A set of aqueous photochemistry bins was appended to a biogeochemically enhanced ocean general circulation model, the

Parallel Ocean Program (POP; Maltrud et al. 1998; Moore et al. 2004), which is embedded in the Community Climate System Model (Drake et al. 2005; Collins et al. 2006). Kinetics are driven by quantities such as organic and zooplankton densities imported from standard, nutrient-limited ecodynamics (Moore et al. 2002). A condensed CO production term j(UVA)(DOM) was defined, where the symbols are merely a photolytic proportionality, UV energy in the A spectral band, and dissolved organic concentration. Photon fluxes were computed following established algorithms for passage through the atmosphere (Leifer 1988; Arrigo et al. 2003), with water column attenuation keyed to empirical depth scales (Johnson and Bates 1996).

The constant j was varied within each simulation to represent uncertainties in multiple photochemical microproperties. Enfolded quantities include quantum yield, chromophoric cross section, and the fraction of light-interacting carbon atoms. Broader sensitivity testing was conducted on a run-by-run basis over 1) the net absorption properties of semilabile organic material, and 2) a multiplicity of removal types. The latter encompassed a fixed large-scale time constant, Q10 constraints placed on microbial consumers, and several potential ecosystem structure dependencies. While global properties of the sea were consulted during mechanism configuration, the majority of analysis was confined to the Pacific. Two north–south cruises conducted there span the entire ocean (Bates et al. 1995). Dominant surface concentration patterns were well represented and included equatorial maxima, fall-off in the gyres, a rebound in temperate zones, and strong seasonal pulses. Based on these results, preferred values could be identified for several parameters. They are recommended here at the very least for use in the central Pacific basin. Our model was tentatively also applied to the full global situation. In this capacity closed budgets were computed, and the fluxes obtained are in accord with other recent exercises (Zafiriou et al. 2003).

The project described has been inspired by the need of ocean and atmosphere photochemical communities for simulations coupled across the sea–air interface. Based on our development, a set of guidelines can be defined for early attempts at the insertion of CO into Earth system models. Ultraviolet radiation responsible for production in surface waters may be transferred in broadband and attenuated using methods from localized studies (e.g., Kettle 2000; Van Hobe et al. 2003). Light absorption may be accomplished by a specified constant portion of model organics (Moore et al. 2002; Moore et al. 2004). Quantum yields and related properties of the microchemical system are treatable in aggregate. Removal by microbes may be parameterized initially as a temperature-dependent time constant consistent with survey data (Johnson and Bates 1996; Zafiriou et al. 2003). Transfer from the ocean to the troposphere is currently well handled by double laminar layer formulations (Wanninkhof 1992). Overall the approach is described by baseline and Q10 scenarios referred to in the tables.

Areas for improvement were listed individually in all the above sections. Ultraviolet fractions have thus far been computed offline, based upon seasonal and geographic trends compiled by aqueous environmental chemistry groups. While the link to system model shortwave radiation has been made directly from the outset, atmospheric attenuation may lack consistency (Houghton et al. 1996; Kettle 2000; Arrigo et al. 2003). True spectral resolution may be required, beginning perhaps with UVB. Uncertainties in water column absorption and the fractionation

of model organics exert considerable influence over our CO. The photochemical behavior of DOM depends on its reaction and bleaching history. Dynamic simulation is indicated for the constituent chromophores (Nelson and Siegel 2002; Christian and Anderson 2002). Related issues are to be found on the removal side of our equations. Results obtained on the ocean periphery are decoherent in a manner that may demand detailed bacterial population dynamics. While loss averaging seems at first blush to be an adequate approximation, a single time constant is unlikely to apply at all scales. Several lines of evidence indicate that ecosystem structure modulates the removal rate. In tropical Pacific studies an anticorrelation was observed against net biological activity (Johnson and Bates 1996), and this can be partially reproduced in our model through grazing controls. Interactive simulation of CO consumers would seem to be in order, but they are very poorly characterized. Complications that are less readily categorized include underprediction in polar waters. The problem is most egregious from 60° to 70°S but may exist elsewhere. Underestimates at high latitudes may indicate poorly resolved sea ice interactions in conjunction with missing dark reactions. Stretching of the microbial consumption time could also be involved (Zafiriou et al. 2003).

Many of the aforementioned challenges will have to be addressed in order for carbon monoxide to be better represented in the ocean general circulation context. Earth system models will demand not only fidelity relative to the present day, but an ability to successfully capture global change effects upon surface ocean photochemistry (Houghton et al. 1996). Geocycling of CO will be influenced during the period of anthropogenic warming by gross radiation field, transport, and ecodynamic alterations. The arguments extend additionally to other small molecules produced within the water column by ultraviolet photolysis. Carbonyl sulfide and the nonmethane hydrocarbons constitute prominent examples (Plass Dulmer et al. 1995; Houghton et al. 1996; Van Hobe et al. 2003). It seems likely that expertise acquired here can be transferred to these substances.

Acknowledgments. The authors thank the U.S. Department of Energy's Office of Science and Biology/Environmental Research SciDAC project for support—SciDAC stands for Scientific Discovery through Advanced Computing.

References

Archer, S. D., F. J. Gilbert, J. I. Allen, J. Blackford, and P. D. Nightengale, 2004: Modeling seasonal patterns of dimethyl sulphide production during 1989 at a North Sea site. *Can. J. Fish. Aquat. Sci.,* **61,** 765–787.

Arrigo, K. R., D. Lubin, G. L. van Dijken, O. Holm-Hansen, and E. Morrow, 2003: Impact of a deep ozone hole on Southern Ocean primary production. *J. Geophys. Res.,* **108,** 3154, doi:10.1029/2001JC001226.

Bates, T. S., K. C. Kelly, J. E. Johnson, and R. H. Gammon, 1995: Regional and seasonal variations in the flux of oceanic carbon monoxide to the atmosphere. *J. Geophys. Res.,* **100,** 23 092–23 101.

Benner, R., 2002: Chemical composition and reactivity. *Biogeochemistry of Marine Dissolved Organic Matter,* D. A. Hansell and C. A. Carlson, Eds., Academic Press, 59–90.

Carlson, C. A., and H. R. Ducklow, 1995: Dissolved organic carbon in the upper ocean of the central equatorial Pacific Ocean 1992: Daily and fine scale vertical variations. *Deep-Sea Res. II,* **42,** 639–656.

——, ——, and A. F. Michaels, 1994: Annual flux of dissolved organic carbon from the euphotic zone in the northwestern Sargasso Sea. *Nature,* **371,** 405–408.

——, H. W. Ducklow, and T. D. Sleeter, 1996: Stocks and dynamics of bacterioplankton in the northwestern Sargasso Sea. *Deep-Sea Res. II,* **43,** 491–515.

Christian, J. R., and T. R. Anderson, 2002: Modeling DOM biogeochemistry. *Biogeochemistry of Marine Dissolved Organic Matter,* D. A. Hansell and C. A. Carlson, Eds., Academic Press, 717–756.

Chu, S., S. Elliott, and M. Maltrud, 2003: Global eddy permitting simulations of surface ocean N, Fe, S cycling: Chemosphere. *Global Change Sci.,* **50,** 223–235.

Collins, W. D., and Coauthors, 2006: The Community Climate System Model (CCSM3). *J. Climate,* **19,** 2122–2143.

Crutzen, P. J., and P. H. Zimmerman, 1991: The changing photochemistry of the troposphere. *Tellus,* **43A,** 136–151.

Doney, S. C., R. G. Najjar, and S. Stewart, 1995: Photochemistry, mixing and diurnal cycles in the upper ocean. *J. Mar. Res.,* **53,** 341–369.

Drake, J. B., P. W. Jones, and G. R. Carr, 2005: Overview of the software design of the Community Climate System Model. *Intl. J. High Perf. Comput. Appl.,* **19,** 177–186.

Dukowicz, J. K., R. D. Smith, and R. C. Malone, 1993: A reformulation and implementation of the Bryan–Cox–Semtner ocean model on the Connection Machine. *J. Atmos. Oceanic Technol.,* **10,** 195–208.

Elliott, S., S. Chu, C. Dean, and D. J. Erickson, 2006: TRACEGAS_MOD: Geochemical processing for low concentration volatiles in the CCSM ocean. *Environmental Science and Environmental Computing,* P. Zannetti, D. Rouson, and S. Elliott, Eds.,Vol. 3, Fiatlux and the Envirocomp Institute, in press.

Erickson, D. J., and J. A. Taylor, 1992: 3-D tropospheric CO modeling: The possible influence of the ocean. *Geophys. Res. Lett.,* **19,** 1955–1958.

Fasham, M. J. R., J. L. Sarmiento, R. D. Slater, H. W. Ducklow, and R. Williams, 1993: Ecosystem behavior at Bermuda station S and ocean weather station India: A general circulation model and observational analysis. *Global Biogeochem. Cycles,* **7,** 379–416.

Hougthon, J. T., L. G. Meira Filho, B. A. Callender, N. Harris, A. Kattenberg, and K. Maskell, Eds., 1996: *Climate Change 1995: The Science of Climate Change.* Cambridge University Press, 572 pp.

Johnson, J. B., and T. S. Bates, 1996: Sources and sinks of carbon monoxide in the mixed layer of the tropical South Pacific Ocean. *Global Biogeochem. Cycles,* **10,** 347–359.

Jones, P. W., P. H. Worley, Y. Yoshida, J. B. White, and J. Levesque, 2005: Practical performance portability in the Parallel Ocean Program. *Concurrency Comput.,* **17,** 1317–1327.

Jones, R. D., and R. Y. Morita, 1984a: Effects of various parameters on carbon monoxide oxidation by ammonium oxidizers. *Can. J. Microbiol.,* **30,** 894–899.

——, and ——, 1984b: Effect of several nitrification inhibitors on carbon monoxide and methane oxidation by ammonium oxidizers. *Can. J. Microbiol.,* **30,** 1276–1279.

Jumars, P. A., 1993: *Concepts in Biological Oceanography.* Oxford University Press, 348 pp.

Kanakidou, M., and Coauthors, 1999: 3-D global simulations of tropospheric CO distributions: Results of the GIM/IGAC intercomparison 1997 exercise. *Chem. Global Change Sci.,* **1,** 263–282.

Kasibhatla, P., M. Heimann, P. Rayner, N. Mahowald, R. G. Prinn, and D. E. Hartley, 2000: *Inverse Methods in Global Biogeochemical Cycles. Geophys. Monogr.,* Vol. 114, Amer. Geophys. Union, 324 pp.

Kettle, A. J., 2000: Comparison of dynamic models for the concentration of a photochemical tracer in the upper ocean. *Mar. Freshwater Res.,* **51,** 289–304.

Leifer, A., 1988: *The Kinetics of Environmental Aquatic Photochemistry: Theory and Practice.* American Chemical Society, 336 pp.

Logan, J. A., M. J. Prather, S. C. Wofsy, and M. B. McElroy, 1981: Tropospheric chemistry—A global perspective. *J. Geophys. Res.,* **86,** 7210–7254.

Longhurst, A., 1998: *Ecological Geography of the Sea.* Academic Press, 398 pp.

Maltrud, M. E., and J. L. McClean, 2005: An eddy resolving global 1/10 degree ocean simulation. *Ocean Modell.,* **8,** 31–54.

——, R. D. Smith, A. J. Semtner, and R. C. Malone, 1998: Global eddy resolved ocean simulations driven by 1985–1995 atmospheric winds. *J. Geophys. Res.,* **103,** 30 825–30 853.

Miller, W. L., O. Calvo-Herrera, and C. Fichot, 2006: Estimating ultraviolet radiation in the surface ocean with SeaUV. *SOLAS Newsletter,* No. 3, Surface Ocean Lower Atmosphere Studies Program, University of East Anglia, 3–4.

Moore, J. K., S. C. Doney, J. Kleypas, D. M. Glover, and I. Y. Fung, 2002: An intermediate complexity ecosystem model for the global domain. *Deep-Sea Res. II,* **49,** 403–462.

——, ——, and K. Lindsay, 2004: Upper ocean ecosystem dynamics and iron cycling in a global model. *Global Biogeochem. Cycles,* **18,** GB4028, doi:10.1029/2004GB002220.

Mopper, K., and D. J. Kieber, 2002: Photochemistry and the cycling of carbon, sulfur, nitrogen and phosphorus. *Biogeochemistry of Marine Dissolved Organic Matter,* D. A. Hansell and C. A. Carlson, Eds., Academic Press, 456–508.

——, X. L. Zhou, R. J. Kieber, D. J. Kieber, R. J. Sikorski, and R. D. Jones, 1991: Photochemical degradation of dissolved organic carbon and its impact on the oceanic carbon cycle. *Nature,* **353,** 60–62.

Nelson, N. B., and D. A. Siegel, 2002: Chromophoric DOM in the open ocean. *Biogeochemistry of Marine Dissolved Organic Matter,* D. A. Hansell and C. A. Carlson, Eds., Academic Press, 547–578.

Parsons, T., and M. Takahashi, 1973: *Biological Oceanographic Processes.* Pergamon Press, 186 pp.

Peacock, S., M. Maltrud, and R. Bleck, 2005: Putting models to the data test: A case study using Indian Ocean CFC-11. *Ocean Modell.,* **9,** 1–22.

Piexoto, J. P., and A. H. Oort, 1992: *Physics of Climate.* American Institute of Physics, 520 pp.

Plass Dulmer, C., R. Koppmann, M. Ratte, and J. Rudolph, 1995: Light nonmethane hydrocarbons in seawater. *Global Biogeochem. Cycles,* **9,** 79–100.

Press, W. H., S. A. Teukolsky, W. T. Vettering, and B. P. Flannery, 1992: *Numerical Recipes in Fortran.* Cambridge University Press, 963 pp.

Sarmiento, J. L., R. D. Slater, M. J. R. Fasham, H. W. Ducklow, J. R. Toggweiler, and G. T. Evans, 1993: A seasonal three dimensional ecosystem model of nitrogen cycling in the North Atlantic euphotic zone. *Global Biogeochem. Cycles,* **7,** 417–450.

Semtner, A. J., 1986: History and methodology of modeling the circulation of the world ocean. *Advanced Physical Oceanographic Numerical Modeling,* J. J. O'Brien, Ed., D. Reidel, 13–37.

Sikorski, R. J., and R. G. Zika, 1993: Modeling mixed layer photochemistry of H_2O_2: Optical and chemical modeling of production. *J. Geophys. Res.,* **98,** 2315–2328.

Springer-Young, M., D. J. Erickson, and T. P. Carsey, 1996: Carbon monoxide gradients in the marine boundary layer of the North Atlantic. *J. Geophys. Res.,* **101,** 4479–4484.

Tomczak, M., and J. S. Godfrey, 1994: *Regional Oceanography: An Introduction.* Pergamon Press, 422 pp.

Van Hobe, M., R. G. Najjar, A. J. Kettle, and M. O. Andreae, 2003: Photochemical and physical modeling of carbonyl sulfide in the ocean. *J. Geophys. Res.,* **108,** 3229, doi:10.1029/2000JC000712.

Wanninkhof, R., 1992: Relationship between wind speed and gas exchange over the ocean. *J. Geophys. Res.,* **97,** 7373–7382.

Wiesenburg, D. S., and N. L. Guinasso, 1979: Equilibrium solubilities of methane, carbon monoxide and hydrogen in water and sea water. *J. Chem. Eng. Data,* **24,** 356–360.

Wise, D. L., and G. Houghton, 1968: Diffusion coefficients of neon, krypton, xenon, carbon monoxide and nitric oxide in water at 10–60°. *J. Chem. Eng. Sci.,* **23,** 1211–1216.

Zafiriou, O. C., S. S. Andrews, and W. Wang, 2003: Concordant estimates of oceanic carbon monoxide source/sink processes in the Pacific yield a balanced global "blue-water" CO budget. *Global Biogeochem. Cycles,* **17,** 1015, doi:10.1029/2001GB001638.

Zepp, R. G., and D. M. Cline, 1977: Rates of direct photolysis in the aquatic environment. *Environ. Sci. Technol.,* **11,** 359–366.